



Title	In-Situ Formation of Ti-Al Alloy Thin Tubes in Iron Bodies
Author(s)	Shitara, Yutaro; Ohmi, Tatsuya; Iguchi, Manabu
Citation	実験力学, 13(Special Issue), s199-s204 <a href="https://doi.org/10.11395/jjsem.13.s199">https://doi.org/10.11395/jjsem.13.s199</a>
Issue Date	2013-07-15
Doc URL	<a href="http://hdl.handle.net/2115/74647">http://hdl.handle.net/2115/74647</a>
Rights	著作権は日本実験力学学会にある。利用は著作権の範囲内に限られる。
Type	article
File Information	J.JSEM 13. s199.pdf



[Instructions for use](#)

## In-Situ Formation of Ti-Al Alloy Thin Tubes in Iron Bodies

Yutaro SHITARA<sup>1</sup>, Tatsuya OHMI<sup>2</sup> and Manabu IGUCHI<sup>2</sup>

<sup>1</sup> Graduate School of Engineering, Hokkaido University, Sapporo, Hokkaido 060-8628, Japan

<sup>2</sup> Faculty of Engineering, Hokkaido University, Sapporo, Hokkaido 060-8628, Japan

(Received 12 January 2013; received in revised form 18 March 2013; accepted 20 April 2013)

### Abstract

A novel process to produce a transition metal alloy thin tube in a dissimilar metal body was examined by modifying the conventional sacrificial-core method. A compound containing titanium powder and a compound with aluminum powder were assembled and shaped into a tube-forming compound wire with concentric layers. An iron powder compact including the tube-forming compound wire was thermally dewaxed and sintered. As a result, a thin tube composed of Ti-Al alloy was directly produced in the iron body.

### Key words

Microreactor, Microchannel, Powder Metallurgy, Titanium, Aluminum, Iron

### 1. Introduction

From the late 90s, the development of microreactors has been actively investigated [1]. The microreactors often utilize microchannels as flow paths for reactive fluids and reaction space. The microchannel structure provides a vast specific surface area and a high heat transfer coefficient [2], and therefore allows fast and precise temperature control during reactions in open reactor systems. This indicates that the microreactors are very suitable for catalytic reactions.

The metallic microreactors in particular have drawn attentions for high temperature catalytic reactions because they excel in heat conductivity, high-temperature strength, thermal shock resistance and formability. In fact, previously various kinds of metallic microreactors for catalytic reactions have been reported. For instance, Rebrov *et al.* [3] reported a stainless steel microreactor for the selective catalytic reduction of nitric oxide with ammonia catalyzed by a zeolite. Aartun *et al.* [4] described catalytic conversion of propane to hydrogen in Fe-Cr-Al alloy microreactors with Ni or Rh catalyst, where they utilized a porous alumina film on the alloy substrate produced by high temperature oxidation as the catalyst support. Pfeifer *et al.* [5-6] examined aluminum microreactors with PdZn or Cu catalysts for methanol steam reforming. Schimpf *et al.* [7] experimented with heterogeneously catalyzed gas phase hydrogenation of acrolein by Ru catalyst in carbon-coated microstructured reactors made of an Al-Mg alloy. The foregoing metallic microreactors were fabricated by means of precision mechanical machining, photoetching, micro-electro discharge machining, laser or electron beam machining and galvanization [8]. These surface fabrication techniques, however, need additional treatments such as soldering or bonding to join the grooved workpieces into the three-dimensional microchannels. Such processes will lead to

extended processing time and more operating cost. The establishment of a novel microchannel-fabrication process is therefore of great importance to put the metallic microreactors into more practical application.

We have recently investigated a powder metallurgical microchanneling process using a sacrificial-core method for producing the metallic microchannel devices [9-12]. In this process, two kinds of metals are used: a body metal and a sacrificial-core metal. The former has a higher melting point and is to compose the device body, and the latter is to flow out and give the shape of the microchannel. A body-metal compact containing a shaped sacrificial-core metal is sintered at temperatures between the melting points of these metals. The molten sacrificial-core metal migrates into the body metal powder region by infiltration or diffusion. Then these metals produce an alloy lining layer surrounding the cavity formed at the site initially occupied by the sacrificial core. Some of the lining layers fabricated by this method have been expected to produce catalysts or catalyst supports in the devices [13-16]. A notable feature of the process is that the body metal plays two roles at a time; one is a constitutional material of the device body, and the other is an element of the lining layer. This mechanism thus enables in-situ formation of a set of microchannel and its lining layer. However, it is

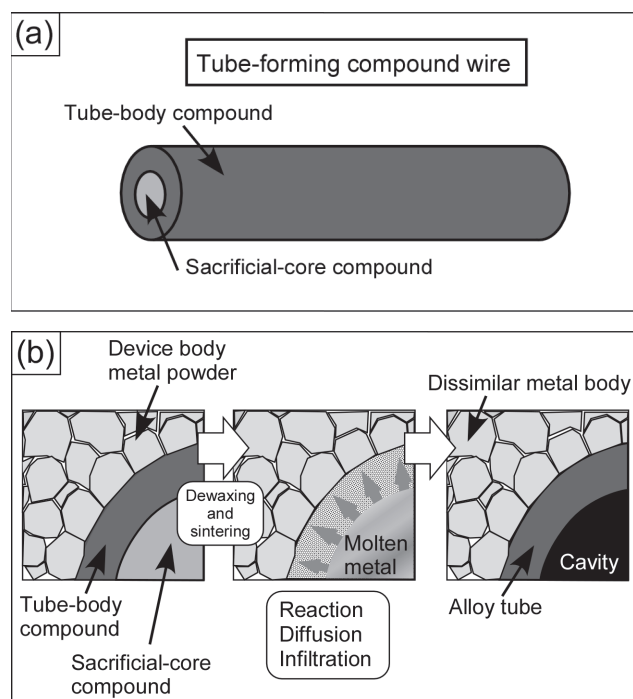


Fig. 1 Constitution of the tube-forming compound wire (a) and schematic representation of the in-situ tube-forming process (b)

difficult to arbitrarily combine the constructional material of the device body and the lining layer composition, which determines the function of the inner wall of the microchannel.

In this study, we hence propose a novel method to produce a transition metal alloy thin tube in a dissimilar metal body. Figure 1 depicts the concept of the process. In this process, a tube-forming compound wire composed of a concentric layer of a tube-body compound and a sacrificial-core compound is used instead of the sacrificial-core metal wire in the conventional sacrificial-core method. Each compound consists of mixture of a metal powder and an organic binder. A powder compact of a dissimilar metal, here defined as a device body metal, containing the tube-forming compound wire is dewaxed and then sintered at temperatures between the melting points of the tube-body metal and the sacrificial-core metal. As a result, a long thin cavity and an alloy lining layer surrounding it are directly produced in the dissimilar metal body. This process will offer greater flexibility in the device design. Moreover, the process will also contribute to saving materials as represented by rare metals such as nickel, which had been often used as the body metals in our previous studies.

As a first step of the study to develop our new process, we chose iron, titanium and aluminum as the device-body metal, the tube-forming metal and the sacrificial-core metal, respectively. At first we examined the feasibility of tube formation, and then observed the tube-formation behavior during heat treatment as well as investigated the effect of high-temperature holding on the composition change of the tube body.

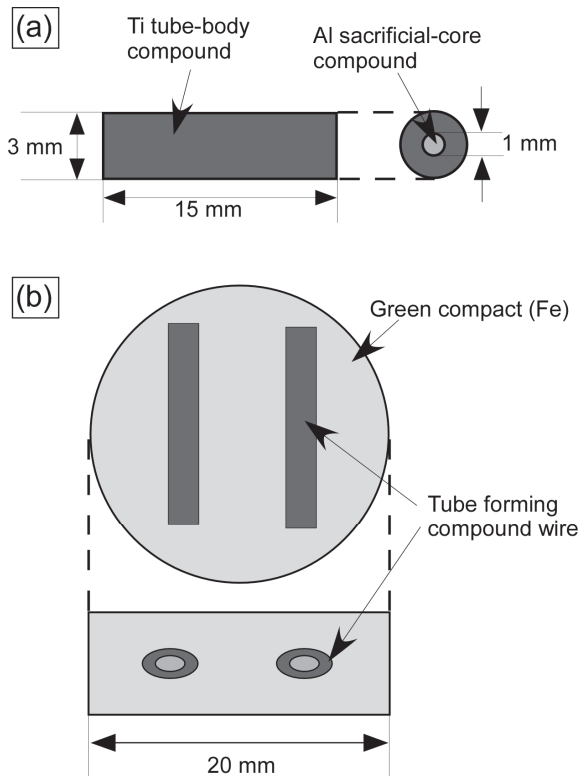


Fig. 2 Schematic illustration of the tube-forming compound (a) and the green compact (b)

## 2. Experimental Procedure

### 2.1 Preparation of specimens

Figure 2 shows schematics of the tube-forming compound wire and the powder compact. In the experiment, titanium powder and aluminum powder were used as the starting materials of the tube-body compound and the sacrificial-core compound, respectively. Each metal powder was mixed with an organic binder in equal volume to obtain the corresponding compound. The organic binder was prepared from yellow wax and pine resin blended in a mass ratio of 1:1. These two compounds were assembled and shaped into a thin pencil-like-form (see Fig. 2 (a)). The tube-forming compound part was about 3 mm in outer diameter and 15 mm in length, and the Al sacrificial-core compound part was about 1 mm in diameter. Two tube-forming compound wires were then included in an iron powder of 13 g and unidirectionally compressed under a given pressure of 624 MPa, thereby a cylindrical green compact of iron containing the Ti/Al tube-forming compound wires was produced as seen in Fig. 2 (b).

### 2.2 Heat treatments

The compact specimens were heat-treated with several heating patterns illustrated in Fig. 3 under an argon atmosphere. The temperature holding time at 573 K for 3.6 ks corresponds to the thermal dewaxing process to clear the organic binder from the tube-forming compound wires in the specimens. Patterns (1), (2) and (3) were used to examine the feasibility of tube formation and the effect of high-temperature holding at 1473 K on the composition change of the tube body. Patterns (A), (B) and (C), on the other hand, were employed to observe the tube formation behavior. In the latter three patterns, the specimens were quenched from each point during heat treatments: the end point of thermal dewaxing (A), 5 K above the melting point of Al (B) and just before high-temperature holding at 1473 K (C). The quenching operations were carried out by dipping in a molten Wood's metal. A green compact without heat treatment was also prepared to check the condition of the specimen before heat treatment.

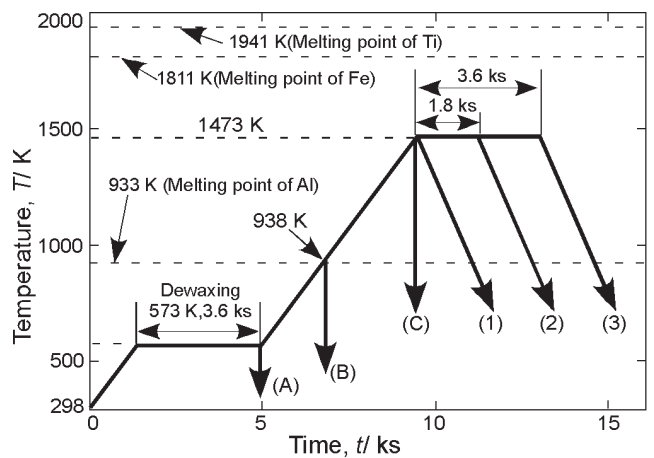


Fig. 3 Heating patterns

### 3. Results and Discussion

#### 3.1 Cavity formation

Figure 4 shows a cross-sectional structure of the thin tube in the specimen heat-treated with Pattern (1). The cross section of the tube was an elliptical shape due to unidirectional pressing during powder compaction. As seen in Fig. 4, a cavity was formed at the original Al sacrificial-core part. The tube was composed of an outer porous sublayer and an inner solid sublayer. EPMA analysis revealed that the average composition of the inner solid sublayer was Al-44.8mol%Ti, which corresponds to TiAl intermetallic compound according to the Ti-Al binary alloy phase diagram [17]. The Al concentrations of the outer porous sublayer varied widely among the points; nevertheless, they were at most 15 mol%, which were in the range of Ti-Al solid solution ( $\beta$ -Ti) at 1473 K or in a coexistence region of  $Ti_3Al$  and Ti-Al solid solution ( $\alpha$ -Ti) at room temperature.

Figure 5 presents a longitudinal section of the thin tube in the specimen heat-treated with Pattern (2). In this specimen, the cavity penetrated almost throughout the length of the original tube-forming compound wire. This result indicates that the long thin tubes whose bodies were composed of Ti-Al alloys were directly produced in the iron bodies. The surface structure of the inner wall of the cavity was porous as seen in Fig. 5 (b). The structure of the

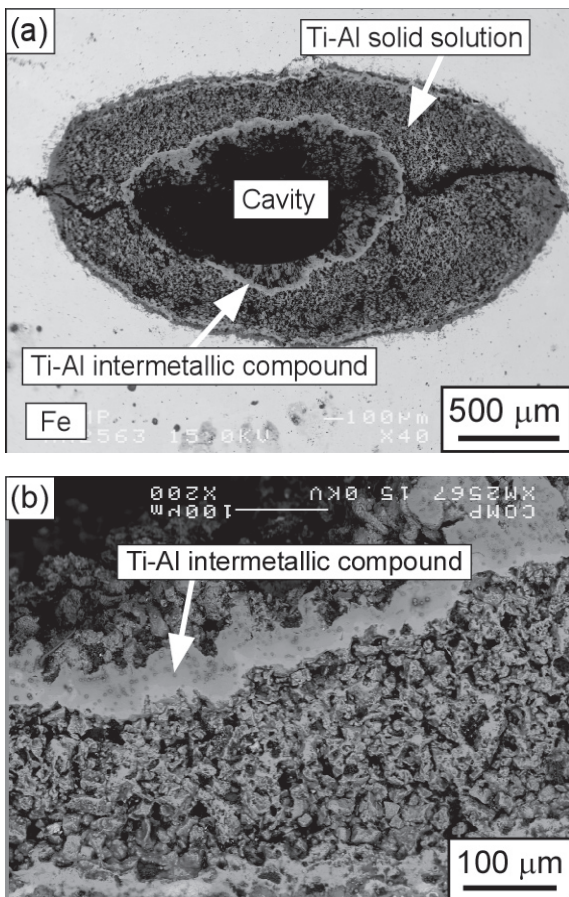


Fig. 4 Back-scattered electron image of a cross-sectional structure of the thin tube in the specimen heat-treated with Pattern (1) (a) and a magnified view of the tube body (b)

thin tube would change depending on the volume fraction of the metal powder in each compound and the mass ratio of the tube-body compound and the sacrificial-core compound.

#### 3.2 Sequence of cavity formation

To clarify the cavity formation behavior, structures of the specimens heat-treated with Patterns (A), (B) and (C) were observed in addition to the specimen without heat treatment.

Figure 6 shows a cross-sectional structure of the tube-forming compound wire in the specimen before heat treatment. The concentric layer structure of the Ti tube-body compound and the Al sacrificial-core compound had been conserved.

Figure 7 provides a structure of the specimen heat-treated with Pattern (A): the specimen was quenched just after thermal dewaxing at 573 K for 3.6 ks. The structure of the dewaxed tube-forming compound was protected with resin. In this specimen, each metal powder formed partially sintered powder networks, in which the metal powder particles three-dimensionally connected each other in corresponding compound regions.

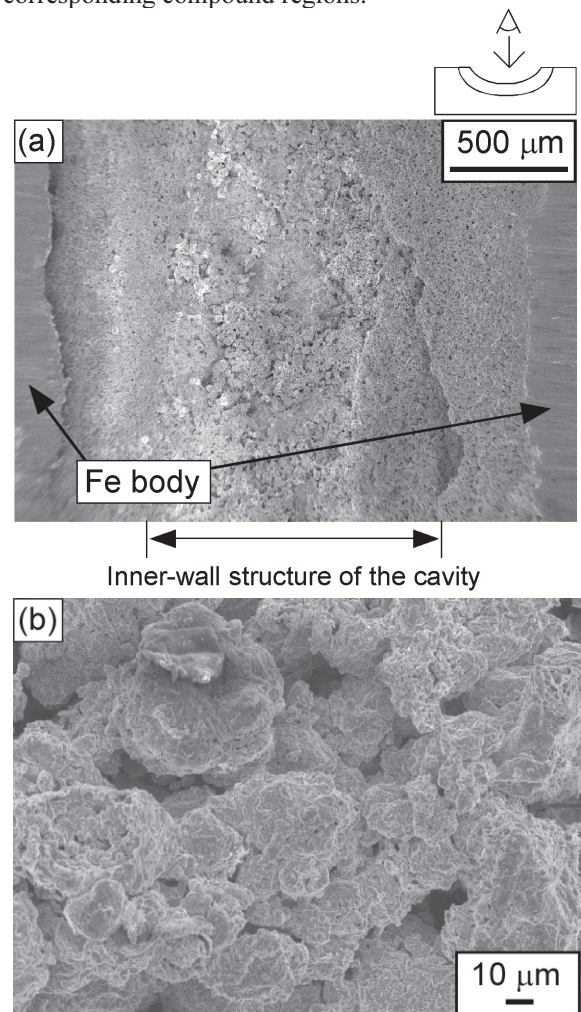


Fig. 5 SEM image of the longitudinal section of the thin tube produced in the specimen heat-treated with Pattern (2) (a) and a magnified view of the inner-wall structure of the cavity (b)

Figure 8 depicts a cross-sectional structure of the specimen quenched at 938 K, 5 K above the melting point of Al (Pattern (B)). In this specimen, the Ti part contained almost no Al. Most of molten aluminum was thus inferred to remain in the sacrificial-core region.

Figure 9 shows a structure of the specimen heat-treated with Pattern (C). The specimen was quenched at 1473 K. The cavity formation had nearly completed in this cross section, however, a partially closed cavity was also observed on another cut plane of the same specimen. This quenching point thus corresponds to the late stage of the cavity formation process. These results suggest that the cavity formation in our novel process was nearly completed at 1473 K and certain tube formation was ensured as seen in Fig. 5 when the specimen was held at 1473 K for up to 1.8 ks.

The time for cavity formation in this process was relatively shorter than that in our previous study on channel formation in an injection-molded tubular compound [18]. The compound specimen was composed of a body compound containing SUS304 stainless steel powder and a sacrificial-core compound with copper powder. In this previous case, we confirmed thin channel

formation in the specimen held at 1473 K for 3.6 ks. When the holding time was less than 3.6 ks, on the other hand, the infiltration of Cu into the SUS304 powder region was not completed. We then discovered that decomposition products generated from the organic binder, mainly composed of C, were main obstacle to the infiltration of Cu, and long high-temperature holding was required to carry them away from the surface of the infiltration paths in the body metal region. Also in the present study, small amount of C was detected by EPMA in the dewaxed specimen since the same organic binder was employed. However, the cavity formation was completed sooner than the previous case. This is attributed to the fact that a certain amount of organic binder was squeezed out of the compound to the iron powder region during powder compaction, and the metal powders were hence more closely packed, increasing their volume fraction in the compound. Actually, image analysis revealed that the volume fraction of the metal powder in the compound wire shown in Fig. 6 was 63.7 %, which was larger than the initial volume fraction, 50 %. In order to examine the adequacy of this factor, we applied the novel in-situ tube formation process to the Fe/SUS304/Cu system. In other words, we prepared an

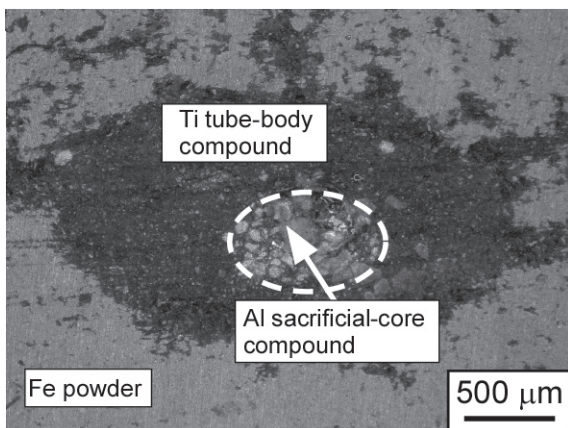


Fig. 6 Optical micrograph of a cross section of the tube-forming compound wire in the specimen before heat treatment

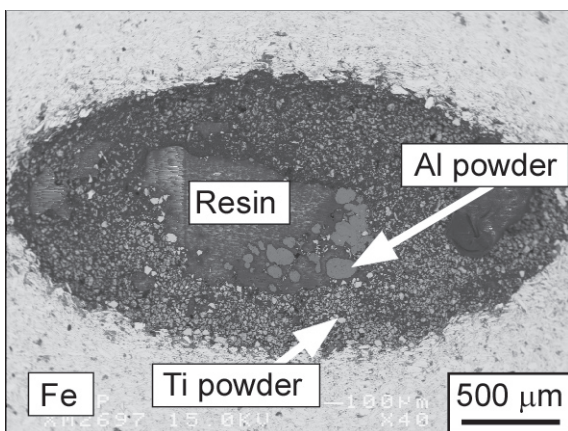


Fig. 7 Back-scattered electron image of a cross-sectional structure of the tube-forming compound wire in the specimen heat-treated with Pattern (A)

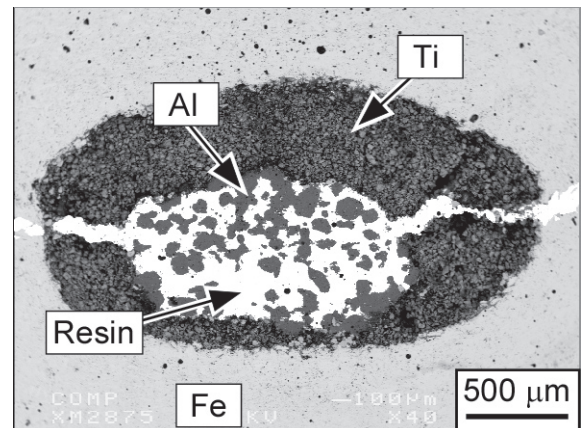


Fig. 8 Back-scattered electron image of a cross-sectional structure of the tube-forming compound wire in the specimen heat-treated with Pattern (B)

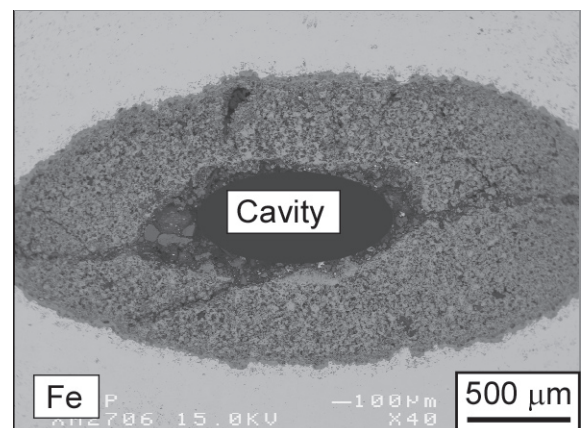


Fig. 9 Back-scattered electron image of a cross-sectional structure of the thin tube in the specimen heat-treated with Pattern (C)

iron powder compact including a tube forming compound wire whose tube body part and sacrificial-core part contain SUS304 and Cu powder, respectively, and tried to form a thin tube in the iron sinter. The mass ratio of the metal powders and the organic binder and the dimensions of the tube-forming compound part were the same as those described in 2.1. The specimen was heat-treated with Pattern (1) in Fig. 3.

Figure 10 shows a cross sectional structure of the SUS304-Cu thin tube produced in the iron sinter. As seen in Fig. 10 (a), a smooth circular cavity was formed at the original Cu sacrificial-core part, and penetration of the cavity was confirmed in this specimen. In Fig. 10 (b), Cu is infiltrated and dispersed in the SUS304 tube body. This indicates that liquid Cu immediately infiltrated into the powder SUS304 region, and the effect of the decomposition products from the organic binder seemed to be reduced due to squeezing of the organic binder during powder compaction. Furthermore, this result suggests that the present process would be able to be applied even to other metal combinations.

### 3.3 Effects of high-temperature holding on the composition of the tube body

Figures 11 and 12 depict cross-sectional structures of the Ti-Al thin tubes in the specimens treated with Patterns (2) and (3): different holding times of 1.8 ks and 3.6 ks, respectively. Compared to the cross-sectional structure shown in Fig. 4, the inner solid sublayer consisting of Ti-Al intermetallic compound tended to disappear as the high-temperature holding time became longer. This suggests that Al in the inner sublayer diffused outwardly during high-temperature holding. We thus focused on the average-concentration changes of Ti and Al near the inner wall of the tube; we defined the regions within about 50 μm outward from the edges of the cavity as the measurement points in each specimen. Figure 13 illustrates the

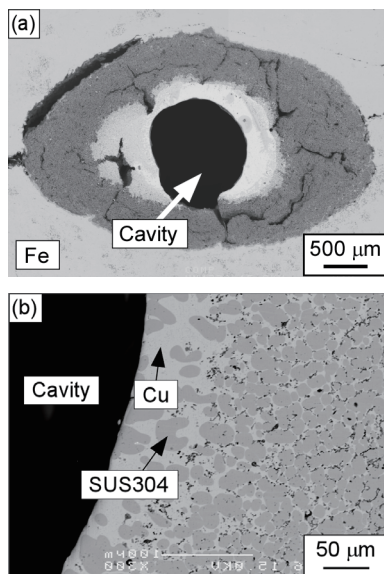


Fig. 10 Back-scattered electron image of a cross section of the Fe/SUS304/Cu specimen (a) and a magnified view of the SUS304-Cu tube body (b)

relationship between the high-temperature holding time and the molar ratio of Ti and Al, expressed as  $C_{Al}/C_{Ti}$ , near the inner walls of the thin tube (the result of Pattern (C) is also shown for comparison). As seen in this figure,  $C_{Al}/C_{Ti}$

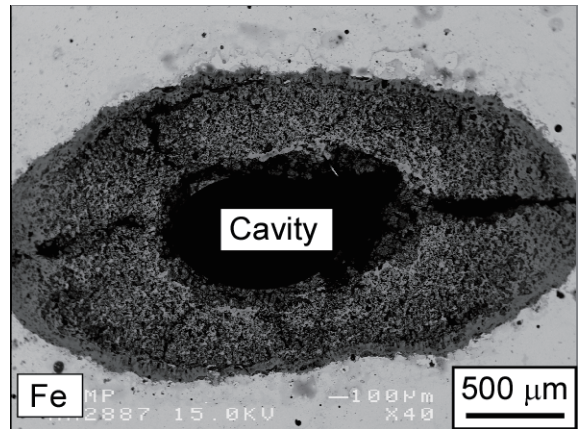


Fig. 11 Back-scattered electron image of a cross-sectional structure of the thin tube in the specimen heat-treated with Pattern (2)

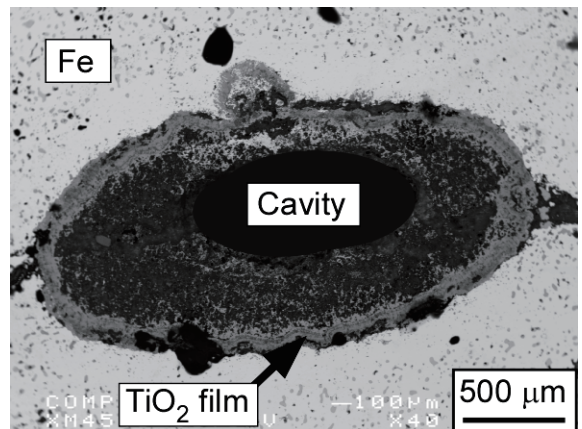


Fig. 12 Back-scattered electron image of a cross-sectional structure of the thin tube in the specimen heat-treated with Pattern (3)

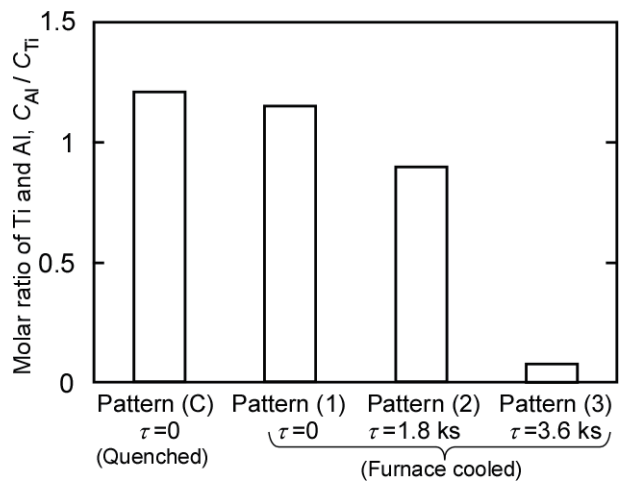


Fig. 13 Relationship between the high-temperature holding time,  $\tau$  and the molar ratio of Ti and Al,  $C_{Al}/C_{Ti}$  near the inner walls of the thin tube

was at peak in the specimen quenched at 1473 K (Pattern (C)), and a similar ratio was detected in the case of Pattern (1). These molar proportions correspond to TiAl intermetallic compound. The Al molar fraction then decreased along with high-temperature holding time as seen in the cases of Patterns (2) and (3). In the specimen treated with Pattern (3),  $C_{Al}/C_{Ti}$  was 0.085, which approximately corresponded to that in the original tube-forming compound.

Meanwhile growth of a thick film circumscribing the tube body was observed in the cases of relatively long holding times such as Patterns (2) and (3). By EPMA analysis, the thick film was revealed to be titania ( $TiO_2$ ). The titania film was probably formed since the outer part of the titanium tube body preferentially reacted with oxygen initially contained in the organic binder. Development of a method to avoid the formation of this oxidation layer is our future issue. Seen from another point of view, however, the titania thick film has a potential to act as a useful barrier between the iron device body and the Ti-Al alloy tube. In other words, it would separate the alloy tube and the dissimilar metal body to prevent interdiffusions among the phases, allowing more strict composition control of the tube body.

#### 4. Conclusions

We have examined the feasibility of a novel process to produce a metal alloy thin tube in a dissimilar metal body by modifying the conventional sacrificial-core method. We used titanium, aluminum and iron for the tube-body compound, the sacrificial-core compound and the device body, respectively. Major findings obtained are summarized as follows:

- (1) A Ti-Al alloy thin tube was directly formed in the iron body when the iron powder compact with tube-forming compound wire was heated and held at 1473 K for more than 1.8 ks.
- (2) The tube body was initially composed of the inner solid sublayer of Ti-Al intermetallic compound and the outer porous sublayer. The composition of the tube body was homogenized by high-temperature holding.
- (3) Growth of the titania film was observed on the circumference of the tube bodies in the specimens held at 1473 K for 1.8 ks and 3.6 ks.

#### References

- [1] Jähnisch, K., Hessel, V., Löwe, H. and Baerns, M.: Chemistry in Microstructured Reactors, *Angew. Chem. Int. Ed.*, **43** (2004), 406-446.
- [2] Kiwi-Minsker, L. and Renken, A.: Microstructured reactors for catalytic reactions, *Catalysis Today*, **110**(2005), 2-14.
- [3] Rebroy, E. V., Seijger, G. B. F., Calis, H. P. A., de Croon, M. H. J. M., van den Bleek, C. M. and Schouten, J. C.: The preparation of highly ordered single layer ZSM-5 coating on prefabricated stainless steel microchannels, *Applied Catalysis A: General*, **206** (2001) 125-143.
- [4] Aartun, I., Gjervan, T., Venvik, H., Görke, O., Pfeifer, P., Fathi, M., Holmen, A. and Schubert, K.: Catalytic conversion of propane to hydrogen in microstructured reactors, *Chem. Eng. J.* **101** (2004) 93-99.
- [5] Pfeifer, P., Schubert, K., Liauw, M. A. and Emig, G.: PdZn catalysts prepared by washcoating microstructured reactors, *Applied Catalysis A:General*, **270** (2004) 165-175.
- [6] Pfeifer, P., Schubert, K. and Emig, G.: Preparation of copper catalyst washcoats for methanol steam reforming in microchannels based on nanoparticles, *Applied Catalysis A:General*, **286** (2005) 175-185.
- [7] Schimpf, S., Bron, M. and Claus, P.: Carbon-coated microstructured reactors for heterogeneously catalyzed gas phase reactions: influence of coating procedure on catalytic activity and selectivity, *Chem. Eng. J.* **101** (2004) 11-16.
- [8] Hosokawa, K.: Microreactors, Epoch-making Technology for Synthesis (in Japanese), ed. by Yoshida, J., CMC Publication, Tokyo, (2003) 37-46.
- [9] Ohmi, T., Takatoo, M., Iguchi, M., Matsuura, K. and Kudoh, M.: Powder-Metallurgical Process for Producing Metallic Microchannel devices, *Mater. Trans.* **47** (2006), 2137-2142.
- [10] Ohmi, T., Hayashi, N. and Iguchi, M.: Formation of Porous Intermetallic Thick Film by Ni-Al Microscopic Reactive Infiltration, *Mater. Trans.*, **49** (2008), 2723-2727.
- [11] Ohmi, T., Takatoo, M. and Iguchi, M.: Powder-Metallurgical Free-Form Microchanneling Process for Producing Metallic Microreactors, *J.JSEM*, **9** (2009), 125-129.
- [12] Ohmi, T., Kodama, T. and Iguchi, M.: Formation Mechanism of Microchannels and Lining Layers in Sintered Iron Powder Compacts with Copper Sacrificial cores, *Mater. Trans.*, **50** (2009), 2891-2896.
- [13] Ishida, M., Ohmi, T., Sakairi, M. and Iguchi, M.: Anodization of the Inner Wall of the Microchannel Formed in Sintered Aluminum Body, *J.JSEM*, **11** (2011), SS267-SS271.
- [14] Saitoh, Y., Ohmi, T., Sakairi, M. and Iguchi, M.: Alkali Leaching of Ni-Al Alloy Microchannel Lining Layers, *J.JSEM*, **11** (2011), SS276-SS279.
- [15] Kobayashi, K., Ohmi, T., Sakairi, M. and Iguchi, M.: Dealloying of Cu-Zn Alloy Microchannel Lining Layers for Producing Microporous Catalyst, *J.JSEM*, **11** (2011), SS280-SS283.
- [16] Nagese, Y., Ohmi, T., Yamauchi, A. and Iguchi, M.: Fabrication of Alumina Coating on Ni-Al Alloy Microchannel Wall for Catalyst Supporting, *J.JSEM*, **11** (2011), SS284-SS287.
- [17] Schuster, J. C. and Palm, M.: Reassessment of the Binary Aluminum-Titanium Phase Diagram, *JPEDAV*, **27** (2006), 255-277.
- [18] Shitara, Y., Ohmi, T., Kumagai, T. and Iguchi, M.: Fabrication of Free-Form Channels by a combined process of Metal Injection Molding and Sacrificial-Core Method, *J.JSEM*, **12** (2012), s226-s231.